Submitted to the
XXXIII International Conference on High Energy Physics
July 26 - August 2, 2006, Moscow, Russia

Abstract:

5. QCD hard interactions
7. Electroweak Physics

An NLO QCD and EW analysis of inclusive $e^{\pm}p$ cross-section data from the ZEUS experiment

ZEUS Collaboration

June 2006

Abstract

A NLO QCD analysis on ZEUS jet-production data and inclusive $e^{\pm}p$ cross-section data, including data with polarised electron beams, is presented. The analysis is used to extract the parton distribution functions of the proton and is extended to fit electroweak parameters. The uncertainties on the parton distributions are competitive with those of the global fits, but have the advantage of being determined on a pure proton target. The electroweak analysis allows both the best measurement of M_W in a space-like process and determinations of the vector and axial-vector neutral current couplings which are competitive in precision with those of the LEP experiments.

1 Introduction

Since the advent of HERA, considerable progress has been made in the determination of the parton distribution functions (PDFs) of the proton. Recently it has been possible to perform PDF fits to HERA data alone [1, 2]. The wide kinematic range covered by the HERA DIS data [2–4], as well as their precision, has allowed the determination of PDFs across a broad range of phase space spanned by the fractional proton momentum carried by the struck quark, Bjorken x, and the negative squared four-momentum transfer between the lepton and nucleon, Q^2. In the ZEUS-JETS fit [1] the lower Q^2 high-statistics neutral current e^+p data [5] determined the low-x sea and gluon distributions, whereas neutral current e^+p DIS inclusive jet cross sections [6] and direct photoproduction dijet cross sections [7] were used to constrain the mid- to high-x ($x \approx 0.01 - 0.5$) gluon PDF. The high-Q^2 neutral and charged current (NC and CC) e^+p and e^-p DIS inclusive cross sections [8–12] determined the valence distributions. Since 2003 HERA has been running with polarised e^+ and e^- beams. The present paper reports on a new PDF fit which has been done including new e^-p NC and CC inclusive cross-section data [13, 14] taken with polarised electron beams. There are 78.8 pb^{-1} of data with left-handed beam polarisation, $\mathcal{P} = -0.27$, and 42.7 pb^{-1} of data with right-handed beam polarisation, $\mathcal{P} = +0.33$. These data are all at high-Q^2, ($Q^2 > 200$ GeV^2), and thus they give an improved determination of the PDFs at high-x, particularly for the u-valence distribution, since the cross sections for NC and CC e^-p scattering are both sensitive to the u-valence PDF at high x.

The use of ZEUS data alone eliminates the uncertainty from heavy-target corrections required in global analyses in which the νFe and μD fixed-target data have been used for determining the valence distributions. The PDFs are presented with accounting for uncertainties from correlated systematic errors (as well as from statistical and uncorrelated sources). Performing an analysis within a single experiment has considerable advantages in this respect since global fits have found significant tensions between different data sets [15].

The data are now sufficiently precise to make it worthwhile examining the extent to which HERA can contribute to constraints on the electro-weak (EW) sector of the Standard Model (SM). The strong dependence of the CC cross-sections on the W propagator is used to make an extraction of M_W and G_F, in a space-like process at high scale, $Q^2 \sim 400$ GeV^2. The weak vector and axial-vector neutral current couplings of quarks, v_u, a_u, v_d, a_d can also be determined. In the DIS process the light quarks dominate the cross-sections so such measurements are complementary to the LEP results, where accurate measurements of these couplings are obtained from $c\bar{c}$ and $b\bar{b}$ production. The analysis was considered at the Born level since the electroweak radiative corrections to the a_i and v_i couplings are not significant in the HERA kinematic regime. This paper presents a combined QCD and EW analysis of the data such that the sensitivity of EW parameters to the choice of PDF is automatically accounted for in the fit. The H1 collaboration made a similar analysis [16] of data from HERA-I, the present analysis extends this by exploiting the information from lepton polarisation in the new data.

2 Theoretical Background

The kinematics of deep inelastic lepton-nucleon scattering are described in terms of the variables Q^2, Bjorken x and y, the fractional energy transfer between the lepton and hadron systems. Since CC scattering involves a pure chiral coupling, it is straightforward to allow for polarised beams. At LO in QCD, the CC e^-p cross-section is given by

$$\left.\frac{d^2\sigma^-}{dxdQ^2}\right|_{CC} = (1-\mathcal{P})\frac{G_F^2}{2\pi x}\frac{M_W^4}{(Q^2+M_W^2)^2}x[u+c+(1-y)^2(\bar{d}+\bar{s}+\bar{b})],$$

where the sensitivity to the u-quark at high-x is evident.

The cross-section for NC scattering of polarised lepton beams, with polarisation $\mathcal{P}$, $(e^\pm(\mathcal{P})p \to e^\pm X)$ may be written

$$\left.\frac{d^2\sigma^\pm}{dxdQ^2}\right|_{NC} = \frac{2\pi\alpha^2}{xQ^4}\left[H_0^\pm + \mathcal{P}H_{\mathcal{P}}^\pm\right], \tag{1}$$

with

$$H_{0,\mathcal{P}}^\pm = Y_+F_2^{0,\mathcal{P}} \mp Y_- xF_3^{0,\mathcal{P}} - \frac{y^2}{2}F_L^{0,\mathcal{P}} \tag{2}$$

where, $Y_\pm = 1 \pm (1-y)^2$, and $\mathcal{P} = \dfrac{N_R - N_L}{N_R + N_L}$, where N_R, N_L are the number of right- and left-handed leptons in the beam respectively. In LO QCD, $F_L^{0,\mathcal{P}} = 0$, and

$$F_2^{0,\mathcal{P}} = \sum_i x(q_i + \bar{q}_i)A_i^{0,\mathcal{P}}, \tag{3}$$

$$xF_3^{0,\mathcal{P}} = \sum_i x(q_i - \bar{q}_i)B_i^{0,\mathcal{P}}, \tag{4}$$

where the coefficients A_i^0, B_i^0 for unpolarised beams are given by

$$A_i^0(Q^2) = e_i^2 - 2e_i v_i v_e P_Z + (v_e^2 + a_e^2)(v_i^2 + a_i^2)P_Z^2 \tag{5}$$

$$B_i^0(Q^2) = -2e_i a_i a_e P_Z + 4a_i v_i v_e a_e P_Z^2 \tag{6}$$

and the coefficients for the polarisation terms are given by

$$A_i^{\mathcal{P}} = 2e_i a_e v_i P_Z - 2a_e v_e(v_i^2 + a_i^2)P_Z^2, \tag{7}$$

$$B_i^{\mathcal{P}} = 2e_i a_i v_e P_Z - 2a_i v_i(v_e^2 + a_e^2)P_Z^2. \tag{8}$$

The term in P_Z arises from $\gamma - Z^0$ interference and the term in P_Z^2 arises purely from Z^0 exchange, where P_Z accounts for the effect of the Z^0 propagator, relative to that of the virtual photon, and is given by

$$P_Z = \frac{Q^2}{Q^2 + M_Z^2} \frac{1}{\sin^2 2\theta_W}. \tag{9}$$

The other factors in the expressions are the charge, e_i, and the NC EW vector and axial vector couplings, v_i, a_i for quark flavour, i, and the corresponding couplings, v_e, a_e for the electron.

3 Analysis Method

The inclusive cross-section data used in the fits were reduced double differential cross-sections in x and Q^2 from: NC e^+p scattering [5, 11]; NC e^-p scattering [9]; CC e^+p scattering [8, 12]; and CC e^-p scattering [10]; jet production data [6, 7] and the new polarised electron beam data [13, 14]. In total there were 795 data points from a total luminosity of 112 pb^{-1} from the HERA-I (1994-2000) running period and a total luminosity of 122 pb^{-1} from the HERA-II (2004-2005) running period. Full account has been taken of correlated experimental systematic uncertainties in the HERA-I data using the Offset method, as described in the ZEUS-JETs PDF analysis [1]. The correlated and uncorrelated systematic errors of the HERA-II data are added in quadrature.

The present analysis was performed within the SM conventional paradigm of leading-twist NLO QCD. The applicability of the leading-twist, NLO DGLAP formalism to HERA data was investigated in a previous ZEUS analysis [3], and suitable data cuts were defined. All the present data lie above these cuts.

The QCD predictions for the PDFs were obtained by solving the DGLAP evolution equations at NLO. These equations yield the PDFs at all values of Q^2 provided they are parameterised as functions of x at some input scale Q_0. The programme QCDNUM [17] was used to perform the evolution. The NLO QCD predictions for the structure functions, which enter into the expressions for the cross sections, were obtained by convoluting the PDFs with the QCD coefficient functions appropriate to the process. It is necessary to specify the scheme and scale choice for the calculations. The renormalisation and factorisation scales for the inclusive DIS processes were chosen to be Q. The DGLAP equations were solved in the $\overline{\mathrm{MS}}$ scheme. For heavy-quark production, the general-mass variable flavour-number scheme of Thorne and Roberts (TRVFN) [18] was used in order to interpolate correctly between threshold behaviour and high-scale behaviour for heavy quarks, as discussed in the ZEUS-S analysis [3]. The value of $\alpha_s(M_Z)$ is fixed, $\alpha_s(M_Z) = 0.118$ [19].

PDF	p_1	p_2	p_3	p_4
xu_v	$(2.7 \pm 0.5 \pm 1.2)$	$0.61 \pm 0.05 \pm 0.10$	$4.13 \pm 0.13 \pm 0.17$	$3.2 \pm 1.1 \pm 1.3$
xd_v	$(1.5 \pm 0.3 \pm 0.7)$	$0.61 \pm 0.05 \pm 0.10$	$4.9 \pm 0.7 \pm 0.8$	$3.5 \pm 2.3 \pm 2.3$
xS	$0.73 \pm 0.02 \pm 0.09$	$-0.216 \pm 0.004 \pm 0.017$	$6.8 \pm 0.7 \pm 1.6$	0
xg	$(1.0 \pm 0.1 \pm 0.3)$	$-0.28 \pm 0.02 \pm 0.04$	$10.1 \pm 0.7 \pm 2.4$	$15 \pm 4 \pm 11$

Table 1: *Table of PDF parameters at $Q_0^2 = 7$ GeV^2, as determined from the ZEUS-pol fit. The first uncertainty given originates from statistical and other uncorrelated sources and the second uncertainty is the additional contribution from correlated systematic uncertainties. The normalisation parameters, p_1, for the u and d valence and for the gluon (indicated by the numbers in parentheses) were derived from the fitted parameters via the number and momentum sum-rules. In addition, the p_2 parameters for the u and d valence quarks were set equal, and p_4 for the sea distribution was set to zero, as detailed in the ZEUS-JETS paper [1].*

The PDFs for u valence, d valence, total sea, gluon and the difference between the d and u contributions to the sea, are each parameterised, at $Q_0^2 = 7$ GeV^2, by the form

$$xf(x) = p_1 x^{p_2}(1-x)^{p_3}(1+p_4 x).$$

It was checked that no significant improvement in χ^2 results from the use of more complex polynomial forms or from variation of the value of Q_0^2. There are 11 free parameters describing the input PDF distributions, the details of the parametrisation are given in the ZEUS-JETS paper [1]. This new PDF fit including polarised electron beam data is called the ZEUS-pol PDF fit.

4 Results

4.1 ZEUS-pol PDF fit

The parameter values and their uncertainties for the ZEUS-pol PDF fit are listed in Table 4.1. The quality of fit to the NC and CC reduced cross-section data is shown in Figs. 1 and 2. The PDFs for the ZEUS-pol fit are shown in Fig. 3 compared to those of the ZEUS-JETS fit, at $Q^2 = 10$ GeV^2. The shapes of the PDFs are not changed significantly by the addition of polarised data. In Fig. 4 the uncertainty of the PDFs for fits with and without the new polarised data data are compared. The precision of the high-x PDF distributions is improved compared to the ZEUS-JETS fit, particularly for the u-valence PDF. The level of precision on the high-x valence PDFs is now comparable to that of global fits including fixed target data [3]. The figure also shows the PDF uncertainties of the ZEUS-pol fit at scale $Q^2 = 10,000$ GeV^2, where PDF uncertainties are a vital input to the estimate of precision $W^{\pm}$ and Z^0 cross-sections at the LHC.

4.2 Extraction of electroweak parameters

A series of fits have been made using the same data sets and the same formalism as the ZEUS-pol fit, but with additional EW parameters freed. Firstly, the value of M_W was freed. The result is given in Table 2 together with the value obtained from a similar analysis of H1 data from HERA-I running. The result from the previous ZEUS analysis is also given. This earlier analysis used the shape of the CC differential cross-section data from HERA-I, with a fixed PDF input, hence the uncertainty resulting from the choice of PDF had to be separately evaluated.

Experiment	M_W (GeV)
ZEUS present analysis	$79.1 \pm 0.77(\text{stat}) \pm 0.99(\text{sys})$
ZEUS [12]	$78.9 \pm 2.0(\text{stat}) \pm 1.8(\text{sys}) \pm 2.0(\text{PDF})$
H1 [16]	$82.87 \pm 1.82(\text{stat}) \pm 0.25(\text{sys})$

Table 2: *Values of M_W extracted from ZEUS and H1 CC data*

Secondly, G_F and M_W were freed, and thirdly the SM formalism was not assumed such that the term, $G_F^2 M_W^4/(Q^2 + M_W^2)^2$, was replaced by the more general form, $g^2/(Q^2 + M_W^2)^2$, and g and M_W were freed. The values of these parameters determined from these fits are given in Table 3. They are in good agreement with the SM.

Free EW params	M_W (GeV)	coupling
G_F, M_W	$82.8 \pm 1.5(\text{stat}) \pm 1.3(\text{sys})$	$G_F = (1.127 \pm 0.013(\text{stat}) \pm 0.014(\text{sys})) \times 10^{-5}$ GeV^{-2}
g, M_W	$82.8 \pm 1.5(\text{stat}) \pm 1.3(\text{sys})$	$g = 0.0772 \pm 0.0021(\text{stat}) \pm 0.0019(\text{sys})$

Table 3: *Values of M_W and the couplings, G_F, g (see text) extracted from ZEUS data*

A further series of fits has been performed in which the neutral current axial-vector and vector couplings are freed, in addition to the PDF parameters. The NC couplings of the electron take the values $a_e = -1/2$, $v_e = -1/2 + 2\sin^2\theta_W \sim -0.05$, so that terms involving v_e are small. There will also be suppression of the pure Z^0 terms through the extra factor of P_Z (at least until very large values of Q^2 are reached). Looking at Eqns. 6, 7, 8, it is clear that NC DIS data from unpolarised lepton beams is sensitive to a_i through xF_3^0, whereas data from polarised lepton beams is sensitive to v_i through F_2^P.

Fit	a_u	a_d	v_u	v_d
SM	0.5	-0.5	0.196	-0.346
ZEUS-pol-a_u-v_u	$0.50 \pm 0.04 \pm 0.09$	-0.5	$0.19 \pm 0.06 \pm 0.06$	-0.346
ZEUS-pol-a_d-v_d	0.5	$-0.49 \pm 0.14 \pm 0.28$	0.196	$-0.37 \pm 0.14 \pm 0.16$
ZEUS-pol-a_u-a_d	$0.48 \pm 0.06 \pm 0.10$	$-0.55 \pm 0.10 \pm 0.21$	0.196	-0.346
ZEUS-pol-v_u-v_d	0.5	-0.5	$0.12 \pm 0.10 \pm 0.06$	$-0.47 \pm 0.15 \pm 0.19$

Table 4: *Values of a_u,a_d,v_u,v_d extracted from fits in which two of the NC couplings are set free in addition to the PDF parameters*

Table 4 presents the values of a_u, v_u, a_d, v_d resulting from fits in which two of the NC vector and axial vector couplings were freed. These fits are labelled as ZEUS-pol-a_u-v_u, ZEUS-pol-a_d-v_d, ZEUS-pol-a_u-a_d, ZEUS-pol-v_d-v_d, according to which EW parameters are freed. The uncertainties on the axial-vector and vector couplings are better displayed as contours since the parameters are correlated to each other and the χ^2 surfaces are asymmetric. The upper plot of Fig. 5 shows the contour of a_u vs v_u and the lower plot shows the contour of a_d vs v_d. This figure also compares these contours to those from similar fits in which the new polarised electron beam data were not included (called the ZEUS-JETS-a_u-v_u and ZEUS-JETS-a_d-v_d fits, respectively). The inclusion of polarised data results in a significant improvement in the determination of the v_u and v_d parameters. This is particularly striking for v_u, since the u PDF is better known than the d PDF and the new data contribute further to our knowledge of the u PDF.

The upper plot of Fig. 7 compares the contour of a_u vs v_u from the present analysis to that from a similar analysis of H1 data [16] in which polarised beam data were not included. The contours determined by CDF [20] and by LEP [21], in the light quark sector, are also shown for comparison. The lower plot makes the same comparisons for the contour a_d vs v_d. Clearly the new polarised data make a significant impact on our knowledge of the weak NC vector couplings in the light quark sector..

The HERA data access information on the weak NC couplings in a different way than LEP and CDF. Whereas these experiments access information on the combinations, $a_u^2 + v_u^2$, and, $a_d^2 + v_d^2$, from the couplings to the Z^0, the HERA data access information on a_u, a_d from xF_3^0 and on v_u, v_d from F_2^P, through γ/Z^0 interference. Thus for HERA data we expect stronger correlations between a_u and a_d, and between v_u and v_d, than between the axial and vector couplings within a flavour. The upper plot of Fig. 6 shows the contour of a_u vs a_d and the lower plot shows the contour of v_u vs v_d. This figure also compares these contours to those from similar fits in which the new polarised electron beam data are not included (called the ZEUS-JETS-a_u-a_d and ZEUS-JETS-v_u-v_d fits, respectively). The correlations between the parameters and the improvement in the determination of the v_u and v_d parameters are evident.

Fits have also been made using the SM formalism

$$a_q = T_q^3, \tag{10}$$
$$v_q = T_q^3 - 2e_q \sin^2\theta_W \tag{11}$$

The values of T_u^3, T_d^3 and $\sin^2\theta_W$ were freed, as well as the PDF parameters. Note that $\sin^2\theta_W$ is also present in the P_Z terms, thus providing an extra constraint. The resulting values of the parameters and their uncertainties are given in Table 5. They are consistent with their SM values. The upper plot of Fig 8 shows the contour of T_u^3 vs T_d^3 from this fit. This contour can be compared with the a_u,a_d contour of Fig. 6, illustrating the consistency of these fits.

The SM formalism can be extended to include right-handed isospin as follows,

$$a_q = T_{q,L}^3 + T_{q,R}^3, \tag{12}$$
$$v_q = T_{q,L}^3 - T_{q,R}^3 - 2e_q \sin^2\theta_W \tag{13}$$

A fit was made in which the left handed couplings $T_{q,L}^3$ were fixed to their SM values but the right handed couplings were freed. The value of $\sin^2\theta_W$ was also freed in a further fit. The resulting parameter values and their uncertainties are given in Table 5 and the contour of $T_{u,R}^3$ vs $T_{d,R}^3$ is shown in the lower plot of Fig 8. All parameters are found to be consistent with their SM values.

5 Summary

Due to the precision and kinematic coverage of the ZEUS data, it is now possible to extract proton PDFs in a fit to data from a single experiment with minimal external input. The ZEUS high-Q^2 cross sections have been used to constrain the valence PDFs, ZEUS low-Q^2 NC data have been used to constrain the low-x sea and gluon distributions and ZEUS data on jet production have been used to constrain the mid- to high-x gluon.

Fit	$T^3_{u,L}$	$T^3_{d,L}$	$\sin^2\theta_W$
ZEUS-pol-T^3_u-T^3_d-$\sin^2\theta_W$	$0.47 \pm 0.05 \pm 0.13$	$-0.55 \pm 0.18 \pm 0.35$	$0.231 \pm 0.024 \pm 0.070$
Fit	$T^3_{u,R}$	$T^3_{d,R}$	$\sin^2\theta_W$
ZEUS-pol-$T^3_{u,R}$-$T^3_{d,R}$	$-0.04 \pm 0.06 \pm 0.13$	$-0.14 \pm 0.18 \pm 0.33$	0.2315
ZEUS-pol-$T^3_{u,R}$-$T^3_{d,R}$-$\sin^2\theta_W$	$-0.07 \pm 0.07 \pm 0.07$	$-0.26 \pm 0.19 \pm 0.19$	$0.238 \pm 0.011 \pm 0.023$

Table 5: *Values of $T^3_{u,L}$, $T^3_{d,L}$, $T^3_{u,R}$, $T^3_{d,R}$, $\sin^2\theta_W$ extracted from fits in which some of these parameters are set free in addition to the PDF parameters*

The uncertainties on the valence PDFs are now competitive with those of the global fits, and they are not subject to uncertainties from heavy-target corrections, higher-twist contributions or isospin-symmetry assumptions. The new ZEUS data taken with polarised electron beams have improved our knowledge of the u-valence PDF significantly. These data also enable us to put constraints on the electroweak sector of the Standard Model. A simultaneous fit to the propagator mass M_W and the PDF parameters gives the best measurement of M_W in a space-like process,

$$M_W = 79.1 \pm 0.77(\text{stat.}) \pm 0.99(\text{syst.})\ \text{GeV}$$

The neutral current vector and axial vector couplings have also been determined in a series of simutaneous fits with the PDF parameters. The axial couplings are dominantly constrained by unpolarised data, whereas the new polarised electron beam data provide significant constraints on the vector couplings. These determinations of the neutral current couplings are competitive in precision with those of the LEP experiments in the light-quark sector, and because they derive from $\gamma - Z^0$ interference they do not suffer from the sign ambiguity of the LEP results.

Acknowledgements

We thank the DESY directorate for their strong support and encouragement. The remarkable achievements of the HERA machine group were essential for the successful completion of this work and are greatly appreciated. The design, construction and installation of the ZEUS detector has been made possible by the effort of many people who are not listed as authors. We acknowledge helpful discussions with Robert Thorne and Dick Roberts.

References

[1] ZEUS Coll., S. Chekanov et al., Eur. Phys. J. **C 42**, 1 (2005).

[2] H1 Coll., C. Adloff et al., Eur. Phys. J. **C 30**, 1 (2003).

[3] ZEUS Coll., S. Chekanov et al., Phys. Rev. **D 67**, 012007 (2003).

[4] H1 Coll., C. Adloff et al., Eur. Phys. J. **C 21**, 33 (2001).

[5] ZEUS Coll., S. Chekanov et al., Eur. Phys. J. **C 21**, 443 (2001).

[6] ZEUS Coll., S. Chekanov et al., Phys. Lett. **B 547**, 164 (2002).

[7] ZEUS Coll., S. Chekanov et al., Eur. Phys. J. **C 23**, 615 (2002).

[8] ZEUS Coll., J. Breitweg et al., Eur. Phys. J. **C 12**, 411 (2000).

[9] ZEUS Coll., S. Chekanov et al., Eur. Phys. J. **C 28**, 175 (2003).

[10] ZEUS Coll., S. Chekanov et al., Phys. Lett. **B 539**, 197 (2002).

[11] ZEUS Coll., S. Chekanov et al., Phys. Rev. **D 70**, 052001 (2004).

[12] ZEUS Coll., S. Chekanov et al., Eur. Phys. J. **C 32**, 16 (2003).

[13] ZEUS Coll., *Measurement of high-Q^2 Neutral Current deep inelastic scattering cross sections with a longitudinally polarised e- beam at HERA*. ZEUS Abstract, *XXXIIIrd International Conference on High Energy Physics, Moscow, Russia (ICHEP2006)*, July 2006, 2006.

[14] ZEUS Coll., *Measurement of high-Q^2 Charged Current deep inelastic scattering cross sections with a longitudinally polarised e- beam at HERA*. ZEUS Abstract, *XXXIIIrd International Conference on High Energy Physics, Moscow, Russia (ICHEP2006)*, July 2006, 2006.

[15] A.D. Martin et al., Eur. Phys. J. **C 23**, 73 (2002).

[16] H1 Coll., A. Aktas et al., Phys. Lett. **B 632**, 35 (2006).

[17] M. Botje, *QCDNUM version 16.12* (unpublished), available on `http://www.nikhef.nl/~h24/qcdcode/index.html`.

[18] R.G. Roberts and R.S. Thorne, Phys. Rev. **D 57**, 6871 (1998).

[19] Particle Data Group, S. Eidelman et al., Phys. Lett. **B 592**, 1 (2004).

[20] CDF Coll., D. Acosta et al., Phys. Rev. **D 70**, 032002 (2005).

[21] Aleph Coll., Delphi Coll., L3 Coll., OPAl Coll., SLD Coll., The LEP and SLD Electroweak Working Groups, Phys. Rep. **427**, 257 (2006).

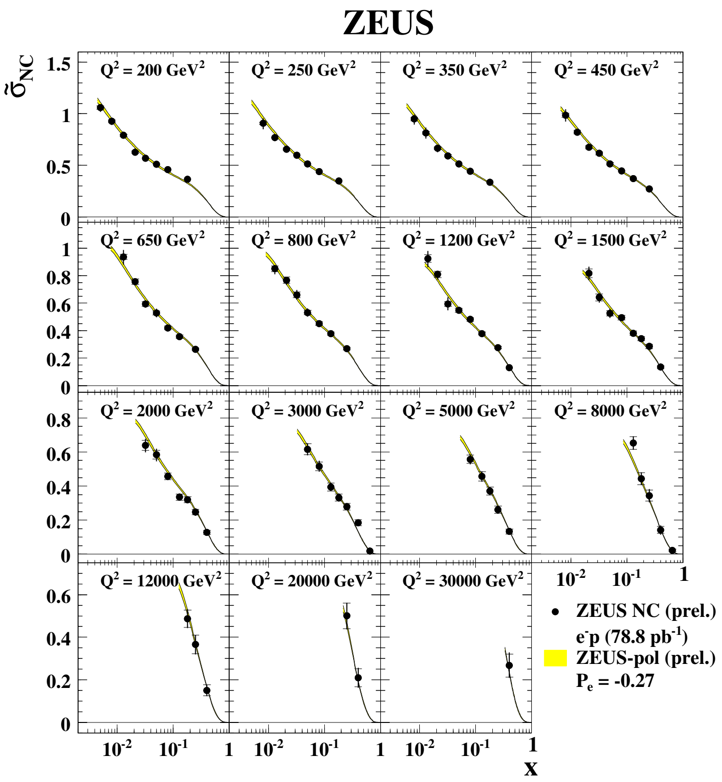

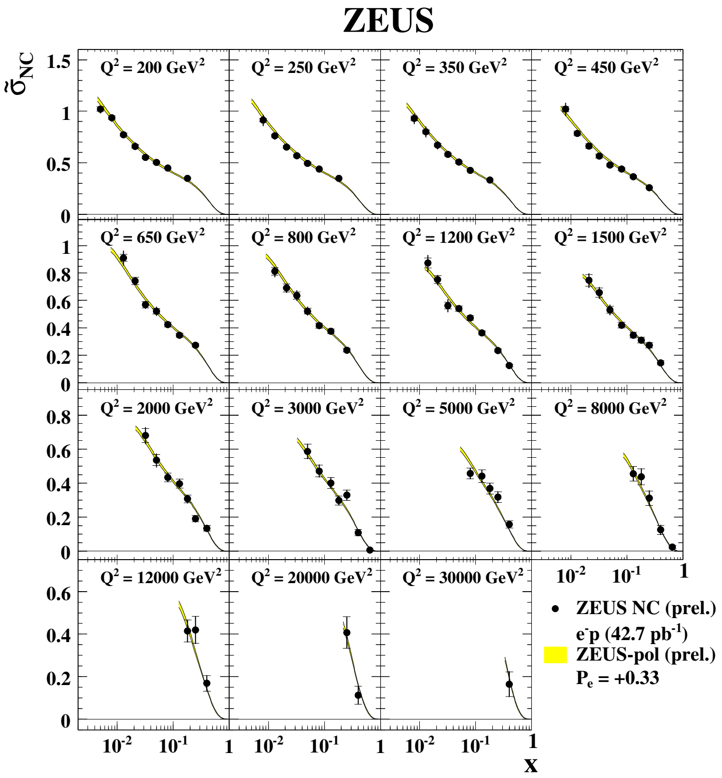

Figure 1: *The ZEUS-pol PDF fit compared to ZEUS e^-p NC reduced cross sections, $\tilde{\sigma}_{\rm NC} = \frac{xQ^4}{2\pi\alpha^2 Y_+}\frac{d^2\sigma}{dxdQ^2}$. Upper plot: for negative beam polarisation. Lower plot: for positive beam polarisation.*

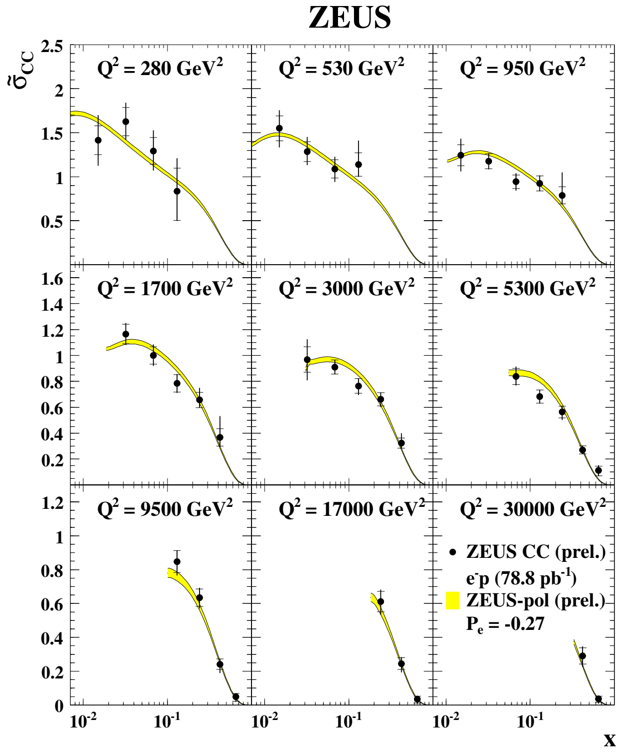

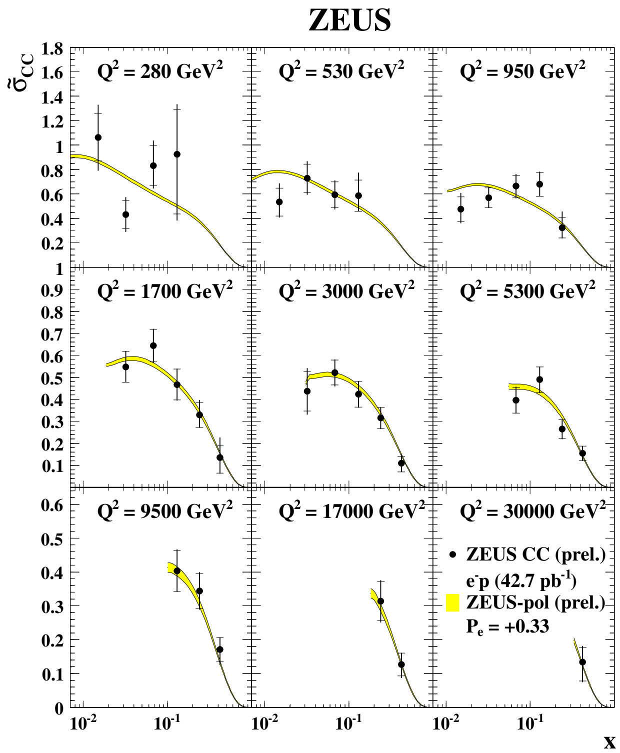

Figure 2: *The ZEUS-pol PDF fit compared to ZEUS e^-p CC reduced cross sections, $\tilde{\sigma}_{\rm CC} = \frac{2\pi x}{G_F^2}\frac{(Q^2+M_W^2)^2}{M_W^4}\frac{d^2\sigma}{dxdQ^2}$. Upper plot: for negative beam polarisation. Lower plot: for positive beam polarisation.*

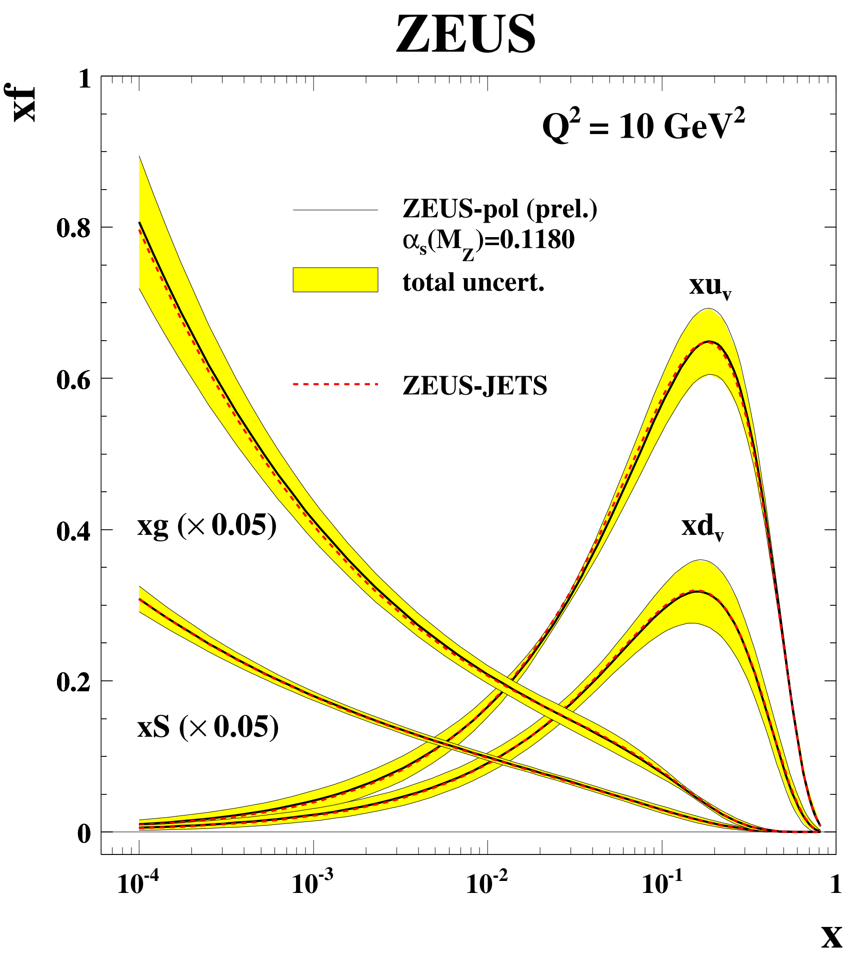

Figure 3: *Comparison of the PDFs extracted from the ZEUS-pol PDF fit with those extracted in the ZEUS-JETS PDF analysis. The ZEUS-pol PDFs are shown together with their total experimental uncertainty, whereas the ZEUS-JETS PDFs are shown by their central values.*

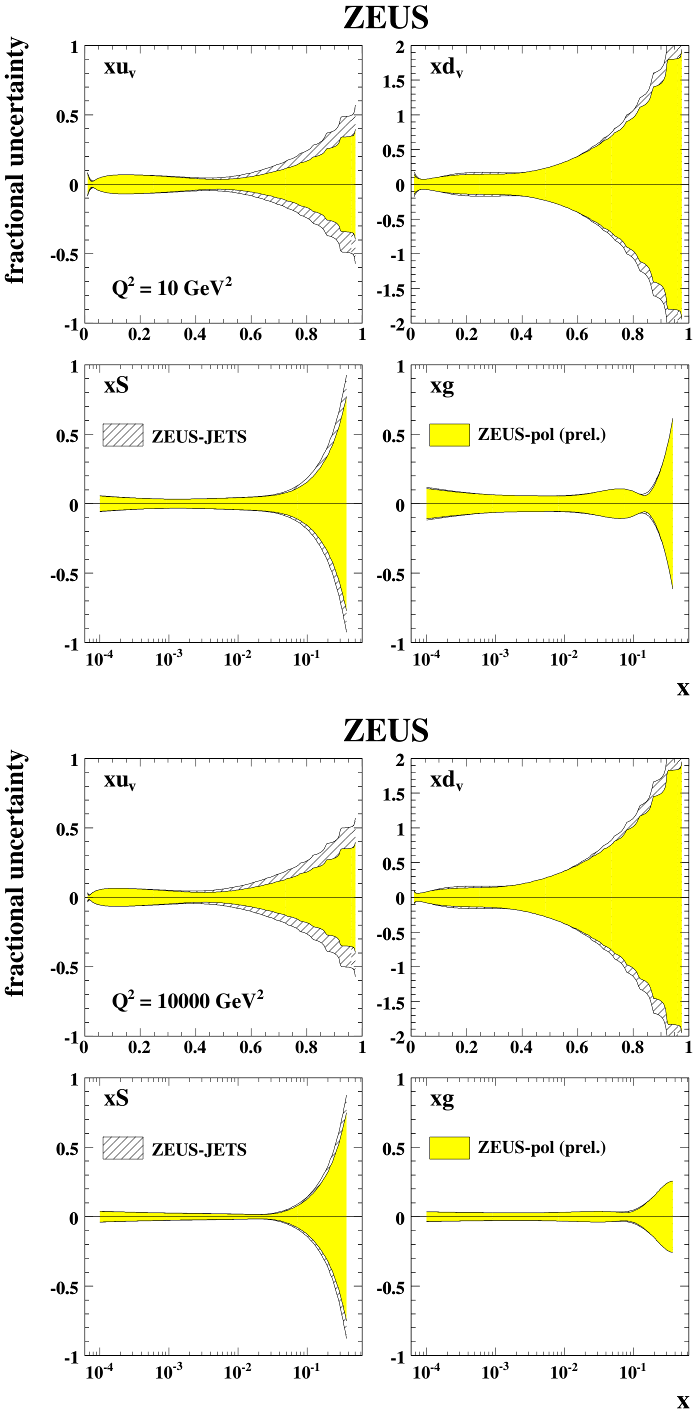

Figure 4: *The total experimental uncertainty on the PDFs at $Q^2 = 10 GeV^2$ (upper plot) and $Q^2 = 10,000 GeV^2$ (lower plot), for the ZEUS-pol fit (central error bands) compared to the total experimental uncertainty on the PDFs for the previous ZEUS-JETS fit (outer error bands). The uncertainties are shown as fractional differences from the central values of the fits. The total experimental uncertainty includes the statistical, uncorrelated and correlated systematic uncertainties and normalisations, for both fits.*

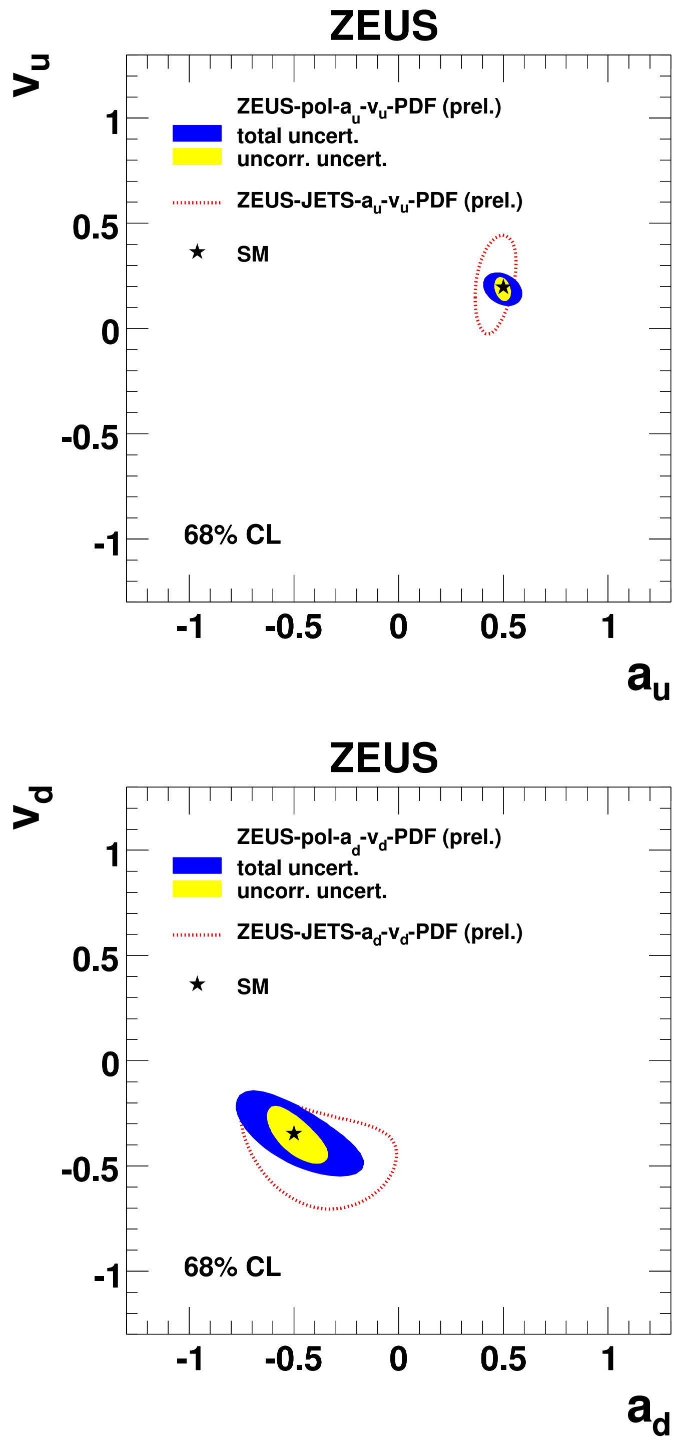

Figure 5: *The 68% confidence level contours for the electroweak parameters a_u vs v_u (upper plot) and a_d vs v_d (lower plot) from the ZEUS-pol-a_u-v_u and the ZEUS-pol-a_d-v_d fit, compared to those from similar fits in which the new polarised data were not included (the ZEUS-JETS-a_u-v_u and ZEUS-JETS-a_d-v_d fits).*

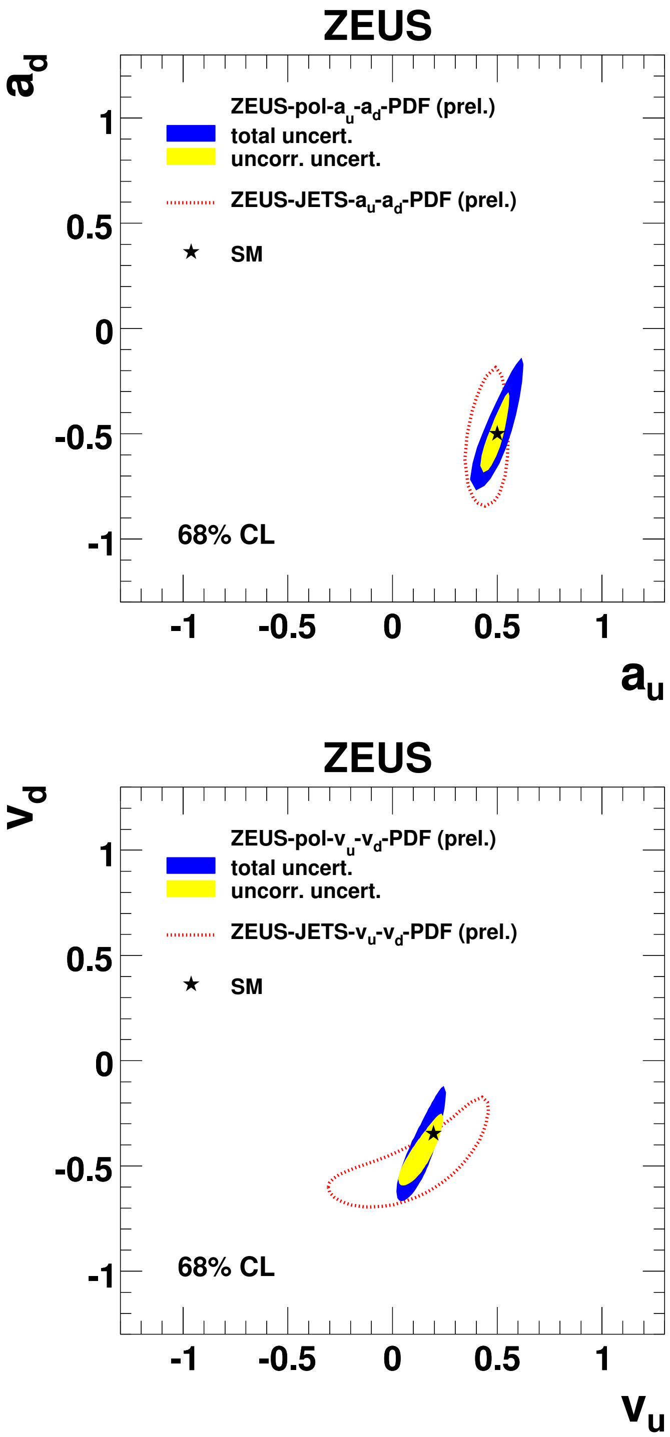

Figure 6: *The 68% confidence level contours for the electroweak parameters a_u vs a_d (upper plot) and v_u vs v_d (lower plot) from the ZEUS-pol-a_u-a_d and the ZEUS-pol-v_u-v_d fit, compared to those from a similar fit in which the new polarised data were not included (the ZEUS-JETS-a_u-a_d and ZEUS-JETS-v_u-v_d fits)..*

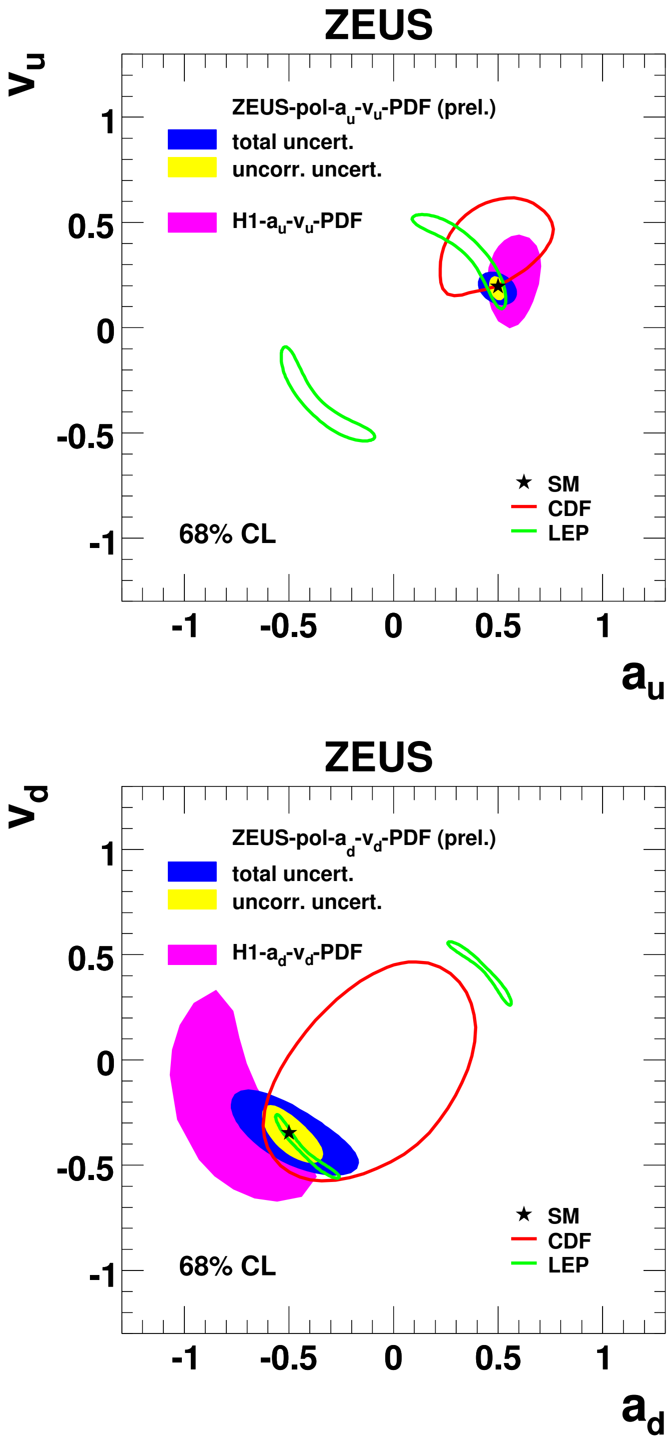

Figure 7: *The 68% confidence level contours for the electroweak parameters a_u vs v_u (upper plot) and a_d vs v_d (lower plot) from the from the ZEUS-pol-a_u-v_u and the ZEUS-pol-a_d-v_d fit, compared to these contours as extracted from other experiments.*

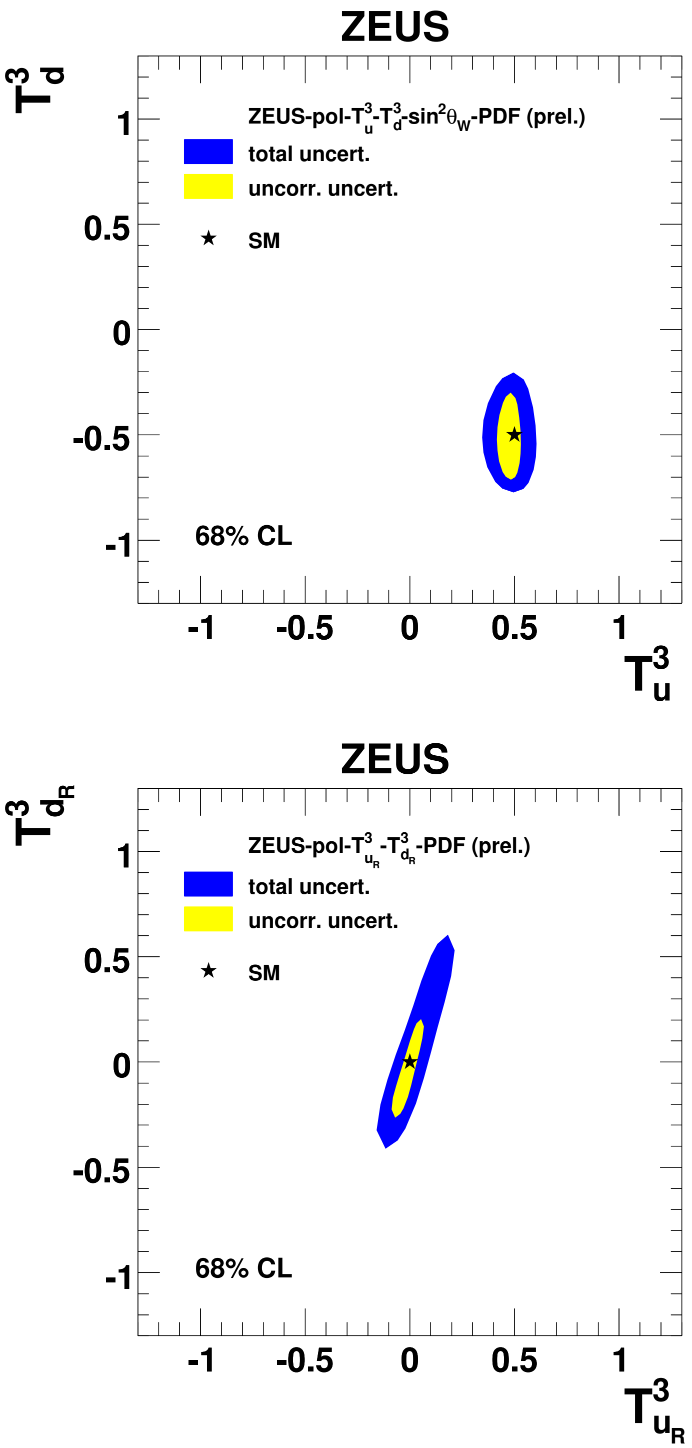

Figure 8: *Upper plot: the 68% confidence level contours for the electroweak parameters T_{3u} vs T_{3d} from the ZEUS-pol-T_{3u}-T_{3d}-$sin^2\theta_w$ PDF fit. Lower plot: the 68% confidence level contours for the electroweak parameters T_{3uR} vs T_{3dR} from the ZEUS-pol-T_{3uR}-T_{3dR} fit.*